

GEOMETRICALLY NON-LINEAR ANALYSIS OF REINFORCED CONCRETE FRAME STRUCTURES WITH THE ACCOUNT OF CREEP AND CRACKING IN THE TENSION ZONE

I. Cypinas & I. Cypinas

To cite this article: I. Cypinas & I. Cypinas (1996) GEOMETRICALLY NON-LINEAR ANALYSIS OF REINFORCED CONCRETE FRAME STRUCTURES WITH THE ACCOUNT OF CREEP AND CRACKING IN THE TENSION ZONE, *Statyba*, 2:8, 11-20, DOI: [10.1080/13921525.1996.10590167](https://doi.org/10.1080/13921525.1996.10590167)

To link to this article: <https://doi.org/10.1080/13921525.1996.10590167>



Published online: 01 Nov 2012.



Submit your article to this journal [↗](#)



Article views: 88

GEOMETRICALLY NON-LINEAR ANALYSIS OF REINFORCED CONCRETE FRAME STRUCTURES WITH THE ACCOUNT OF CREEP AND CRACKING IN THE TENSION ZONE

I. Cypinas

1. Introduction

A number of analytical models and approximate methods are developed to evaluate various secondary factors, influencing the real behaviour of reinforced concrete structures. Some of these methods, such as age-adjusted-effective-modulus (AAEM) method for concrete creep analysis [1], interpolation formulas [2], used to evaluate the contribution of the cracked tension zone to the resistance of a reinforced concrete cross-section, and approximate methods for $P-\Delta$ analysis of a structure [3], are widely used. Each of them proved its validity for the solution of the particular problems. But in the case of coupling of these factors the results may be unexpected, and more consistent analytical models are required.

The creep strain at time t due to variable stress $\sigma(t')$ is represented by the hereditary integral

$$\varepsilon(t) = \sigma(t_0)J(t, t_0) + \int_0^t J(t, t')d\sigma(t'). \quad (1.1)$$

The creep compliance function $J(t, t')$ here is appropriate analytical expression, adjusted to the available experimental data. A number of algebraic relations for this function are proposed [4], [5], [6]. Constitutive relation (1.1) can be extended to the non-linear range, when the stress exceeds the level about $0.4f_c$, where f_c — compressive strength. The authors of [6] recommend the relation that can be presented in the form, analogous to (1.1)

$$\varepsilon(t) = \sigma(t_0)J(t, t_0) + \int_0^t J(t, t')dF[\sigma(t')] \quad (1.2)$$

where $F(\sigma)$ is a certain time-independent function.

Integral-type constitutional relations will be involved in the resulting set of governing structural equations that are obtained by means of finite element techniques. To obtain a numerical solution these

equations must be reformulated in terms of discrete time intervals. Describing the stress history $\sigma = \sigma(t)$ by a broken line, we shall replace the integral relation (1.1) by a finite sum. Then the increment of strain will be written in a concise form as

$$\Delta \varepsilon_i = \frac{\Delta \sigma_i}{E'_i} + \Delta \varepsilon'_i. \quad (1.3)$$

The quasi-elastic modulus E'_i here is

$$\frac{1}{E'_i} = \frac{\Delta \sigma_i}{\Delta t_i} \int_{t_{i-1}}^{t_i} J(t_i, t') dt'. \quad (1.4)$$

The second term in (1.3) $\Delta \varepsilon'_i$ represents the contribution of previously applied stress:

$$\Delta \varepsilon'_i = \sigma_0 \Delta J(t_i, t_0) + \sum_{j=1}^{i-1} \frac{\Delta \sigma_j}{\Delta t_j} \int_{t_{j-1}}^{t_j} \Delta J(t_i, t') dt'. \quad (1.5)$$

Here

$$\Delta \varepsilon_i = \varepsilon(t_i) - \varepsilon(t_{i-1}), \quad \Delta \sigma_i = \sigma(t_i) - \sigma(t_{i-1}), \\ \Delta t_i = t_i - t_{i-1}, \quad \Delta J(t_i, t') = J(t_i, t') - J(t_{i-1}, t'). \quad (1.6)$$

This formulation is known as the so-called memory model of creep [7]. Its disadvantage is large demand of storage space for stress history of each individual member. One can attempt to diminish the data storage, converting the creep compliance function into a series form

$$J(t, t') = \sum_{k=1}^m a_k(t) b_k(t'). \quad (1.7)$$

The increment of strain then will be obtained as

$$\Delta \varepsilon_i = \frac{\Delta \sigma_i}{\Delta t_i} \sum_{k=1}^m a_k(t_i) \int_{t_{i-1}}^{t_i} b_k(t') dt' + \\ \sum_{k=1}^m \Delta a_k(t_i) \int_{t_0}^{t_{i-1}} b_k(t') d\sigma(t'). \quad (1.8)$$

$$\Delta a_k(t_i) = a_k(t_i) - a_k(t_{i-1}). \quad (1.9)$$

The expansion (1.7) represents the so-called state model of creep [7]. The quasi-elastic modulus in this model is represented by the first sum in (1.8). The second sum describes the influence of the stress history. It is obvious that the state model does not exempt from the necessity to store that information. The information about the stress history here is stored in an indirect form, as the integrals in the second sum of (1.8). The two creep models were investigated and compared in [7], but no one showed its decisive advantages.

To avoid the laborious time-stepping procedures, the so-called algebraic methods are used (see, for instance, [8]). Equivalent modulus (EM) method corresponds to the rectangle method of integration with only one step, mean stress (MS) method is an equivalent of trapezium integration method. Age-adjusted-equivalent-modulus (AAEM) method [1] is much more sophisticated. But it rests on the stress mode superposition principle, and therefore hardly can be applied to the non-linear problems.

In recommendations [9], issued by the Moscow Institute of Concrete and Reinforced Concrete, the kernel of the hereditary integral is represented by the series of type of (1.7), with four exponential terms. The creep function has been picked out phenomenologically, using the creep test results. Physically more grounded approach, derived from the so-called solidification theory, is presented by Z. P. Bažant in [10]. The creep compliance function is expanded by the Dirichlet series; the exponential expansion simplifies the numerical solution.

It must be pointed out that concrete in its creep behaviour exhibits rather fading stress memory. Therefore, only the latest stress increments need to be represented in full details, and storage requirements for the memory model may be significantly diminished. The memory model of creep is applied in this paper.

In some recent publications, for instance [11], [12], the tensile stresses of concrete are neglected. However, as far back as in 1984 [13], it was observed that concrete do have significant influence on the creep behaviour of reinforced concrete member in flexure.

The main goal of this research is to formulate the consistent theoretical approach, and to elaborate the appropriate computational procedures that would be able to account for all above mentioned factors at the same time. The finite element computer code, based on the Newton-Raphson algorithm, has been developed and employed to trace the response of the structure in the time domain. The software is applicable to the middle-size planar structural problems.

2. Cracking relations for concrete

If cracks occur in the tension zone of a reinforced concrete member, essential non-linearity is introduced into its behaviour. Non-linear interaction between the tensile reinforcement and adjacent concrete layers is analytically described and investigated in author's previous works [14], [15]. The equivalent strain-softening response of concrete is adopted to represent the contribution of adjacent concrete layers to the resistance of the tensile reinforcement.

The linear creep law (1.1) implies a linear distribution of stress over the compression zone of a cross-section. The cracking behaviour of concrete in the tension zone is described by the analytical stress-strain relation

$$\sigma = f(\varepsilon^s) = \begin{cases} f'_t x, & x = \varepsilon^s / \varepsilon'_t, \text{ if } x \leq 1 \\ f'_t \frac{\beta x}{\beta - 1 + x^\beta}, & \text{if } x > 1 \end{cases} \quad (2.1)$$

that is presented in Fig. 2.1. Here f'_t is the tensile strength of concrete, $\varepsilon'_t = f'_t / E_{sec}$ — the strain, attained at f'_t . The value of β can be computed by the empirical formula [16], based on experimental results. This quantity depends on the parameters of the tensile reinforcement, and the dimensions of the tensile zone. Equation (2.1) approximately summarises the complicated picture of interaction between tensile reinforcement, cracked concrete, and adjacent layers of concrete in an uncracked zone. In the case of ordinary short-time loading the strain ε^s in (2.1), consists of elastic component and the cracking part ξ

$$\varepsilon^s = \sigma / E_{sec} + \xi \quad (2.2)$$

and equation represents the time-independent stress-strain relation.

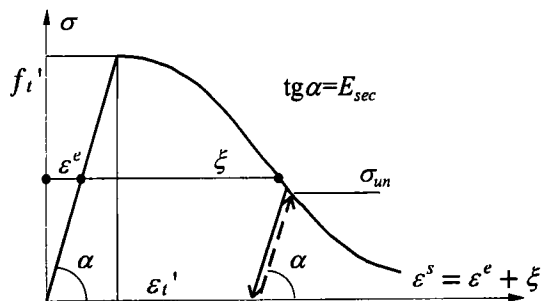


Fig. 2.1. Basic stress-strain relation with the reloading path

The total strain ε in the case of the long-time loading of the tension zone can be analogically divided into a linear creep component ε^c according to the hereditary equation (1.1) and a cracking component ξ :

$$\varepsilon = \varepsilon^c + \xi. \quad (2.3)$$

Equating the quantity ξ in both sums (2.2) and (2.3), we obtain the expression for an argument ε^s of the function (2.1). In this way the main relationship between the long-time strain ε and stress σ can be formulated:

$$\sigma = f(\varepsilon^s),$$

$$\varepsilon^s = \varepsilon - \sigma(t_0)J(t, t_0) - \int_{t_0}^t J(t, t') d\sigma(t') + \frac{\sigma(t)}{E_{sec}}. \quad (2.4)$$

These two equations represent the coupling of creep and cracking strains by the consecutive junction of the non-linear element, modelling the cracking behaviour according to (2.1), and linear creep that follows (1.1). That model of interaction between creep and cracking strains has been presented in reference [17]. In a similar way the interaction between the creep and quasi-brittle response of material in compression after the attainment of peak stress can be modelled [18].

To obtain the long-time relation between σ and ε explicitly, the quantity ε^s must be eliminated from the (2.4). That can be achieved performing time discretisation, in an incremental form, as it was demonstrated previously in [14]. Denoting $E_{tan} = \frac{d\sigma}{d\varepsilon^s}$, and using notations from (1.5) and (1.6), one can formulate the basic incremental constitutional relation of concrete for the i -th time step:

$$\Delta \varepsilon_i = \Delta \sigma_i \left(\frac{1}{E_{tan}} - \frac{1}{E_{sec}} + \frac{1}{E'_i} \right) + \Delta \varepsilon'_i. \quad (2.5)$$

Stress-strain relation (2.1) in its descending branch is valid provided the strain parameter ε^s is growing monotonically. In case of reverse deformation the so-called Bauschinger's effect occurs, as it is shown in Fig. 2.1. We shall consider only small single reverse of strain that usually takes place in the case of the shift of a neutral axis of a cross-section. In the unloading case the tangent modulus in (2.5) becomes $E_{tan} = E_{sec}$ and that equation is reduced to the form of (1.3). This relation also remains valid in case of subsequent reloading until the stress level returns to the unloading point σ_{un} .

3. Finite Element Model

Long-time behaviour of the cracked reinforced concrete cross-section in plane flexure was consistently investigated in [15]. The layer model of a section was introduced in that publication. The use of that model is justified by the non-linear distribution of stress in the cracked zone and prospective extension of the model to the non-linear creep according to (1.2). Numerical procedures to evaluate the stress resultants

$$F = \int_A \sigma dA, \quad M_y = \int_A \sigma z dA \quad (3.1)$$

the incremental section stiffness parameters

$$J_{00} = \int_A \tilde{E} dA, \quad J_{0y} = \int_A \tilde{E} z dA, \quad J_{yy} = \int_A \tilde{E} z^2 dA \quad (3.2)$$

and parameters due to the previous stress action

$$\Delta F^i = \int_A \tilde{E} \Delta \varepsilon^i dA, \quad \Delta M_y^i = \int_A \tilde{E} \Delta \varepsilon^i z dA \quad (3.3)$$

for i -th time step were elaborated in [15]. The modulus \tilde{E} in these formulas corresponds to the quantity in brackets in (2.5) if the concrete is cracked, and $\tilde{E} = E'$ otherwise.

The reference axes here are chosen arbitrarily. Equations, relating section force increments ΔF_i , ΔM_i to the deformation increments during the i -th time interval are obtained in the form

$$\left. \begin{aligned} \Delta F_i &= J_{00} \Delta \varepsilon_i^0 + J_{0y} \Delta \kappa_i^y - \Delta F_i^y, \\ \Delta M_i^y &= J_{y0} \Delta \varepsilon_i^0 + J_{yy} \Delta \kappa_i^y - \Delta M_i^{y,y} \end{aligned} \right\} \quad (3.4)$$

where $\Delta \varepsilon_i^0$ is axial strain increment at the co-ordinate origin point, $\Delta \kappa_i^y$ — curvature increment in regard of y - axis. The right-hand reference system is adopted here, and corresponding sign rule is assumed.

It must be noted that incremental stiffness parameters in (3.4) significantly change in the course of loading, hence, the position of the principal axis in an incremental sense is also being changed. The section stiffness matrix in the equations (3.4), referred to the arbitrary co-ordinate axes, is not diagonal, as a rule. The section stiffness matrix in (3.4), however, can easily be diagonalised for each particular deformation increment by the appropriate shift of the co-ordinate origin point. Then the equations (3.4) will appear in the form

$$\left. \begin{aligned} \Delta F_i &= J_{00} \Delta \overset{\circ}{\varepsilon}_i - \Delta F_i', \\ \Delta \overset{\circ}{M}_i^y &= \overset{\circ}{J}_{yy} \Delta \kappa_i^y - \Delta \overset{\circ}{M}_i'^y \end{aligned} \right\} \quad (3.5)$$

Here $\overset{\circ}{J}_{yy} = J_{yy} - z_c^2 J_{00}$ is incremental section stiffness parameter in regard of centroidal axis, $z_c = J_{0y} / J_{00}$ is the location of centroidal axis for current deformation increment. The increment of the longitudinal strain

$$\Delta \overset{\circ}{\varepsilon}_i = \Delta \varepsilon_i + z_c \Delta \kappa_i^y \quad (3.6)$$

is measured at the centroid of a cross-section. All section integrals now are computed in regard of centroidal axes, so the axial force increments $\Delta F_i, \Delta F_i'$ in (3.5) are applied to the centroid of the section. Moments are equal to

$$\Delta \overset{\circ}{M}_i^y = \Delta M_i^y - z_c \Delta F_i'. \quad (3.7)$$

It must be remembered that in case of varying bending moment the cross-sectional stiffness of the finite element is also variable. Another complication is more intricate. The point is that the term $\Delta F_i'$ in the first of equations (3.5) may be not constant over the length of the finite element even if the stiffness parameters are constant. Indeed, the integral quantity $\Delta F_i'$ in (3.3) depends on the creep strain component $\Delta \varepsilon_i'$, defined by (1.5), as a linear function of the previous stress increments $\Delta \sigma_j$, $j = 1, \dots, i-1$. But in case of asymmetric reinforcement the resultants of

concrete stress increments $\int_A \Delta \sigma_j dA$ will not be constant, if the bending moment is variable. But the axial force increment $\Delta F_i'$ in the left-hand side of (3.5) must be constant owing to the equilibrium condition. Hence, by virtue of (3.5) the axial elongation $\Delta \overset{\circ}{\varepsilon}_i$ in the right-hand side of the equation must also be variable if $\Delta F_i'$ is not constant.

In order to express the variable axial elongation, an additional third node with one degree of freedom has been introduced at a mid-length of the finite element, and quadratic displacement function for axial displacements has been assumed. Variable centroidal strains are obtained

in form of

$$\overset{\circ}{\varepsilon}(x) = \frac{1}{l} \left[u_1 \left(4 \frac{x}{l} - 3 \right) + u_2 \left(4 \frac{x}{l} - 1 \right) - 4u_3 \left(2 \frac{x}{l} - 1 \right) \right]. \quad (3.8)$$

Here l is the length of the element, u_1 and u_2 are the axial displacements of the nodes, and u_3 is the displacement of the additional node. As to the transverse displacements, they are expressed in an usual cubic form, and curvatures of an element are represented by a linear function

$$\begin{aligned} \kappa(x) &= w_1 \left(\frac{6}{l^2} - \frac{12x}{l^3} \right) - \chi_1 \left(\frac{4}{l} - \frac{6x}{l^2} \right) \\ &\quad - w_2 \left(\frac{6}{l^2} - \frac{12x}{l^3} \right) - \chi_2 \left(\frac{2}{l} - \frac{6x}{l^2} \right) \end{aligned} \quad (3.9)$$

where w_1 and w_2 are the displacements in the z -direction of first and second node respectively, χ_1 and χ_2 are rotations of these nodes in the clock-wise direction.

The linearized part of strain is expressed by an ordinary strain-displacement compatibility relation

$$\Delta \overset{\circ}{\varepsilon} = \mathbf{B}(x) \Delta \overset{\circ}{z}. \quad (3.10)$$

Here matrix $\mathbf{B}(x)$ follows from the form functions (3.8), (3.9). Vector of generalised section strains is

$$\Delta \overset{\circ}{\varepsilon} = \{ \overset{\circ}{\varepsilon}(x), \kappa(x) \}^t$$

and the extended nodal displacement vector reads as

$$\Delta \overset{\circ}{z} = \{ u_1, w_1, \chi_1, u_2, w_2, \chi_2, u_3 \}^t.$$

Subsequently, the incremental relation (3.5) for element nodal forces may be represented in a matrix form

$$\Delta \overset{\circ}{\mathbf{F}}_i = \left[\int_L \mathbf{B}^t(x) \overset{\circ}{\mathbf{J}}_i \mathbf{B}(x) dx \right] \Delta \overset{\circ}{\mathbf{z}} - \int_L \mathbf{B}^t(x) \Delta \overset{\circ}{\mathbf{R}}_i dx. (3.11)$$

Here $\overset{\circ}{\mathbf{J}}_i$ is the section stiffness matrix from (3.5), $\Delta \overset{\circ}{\mathbf{R}}_i$ — the vector that consists of the second terms of right-hand side of equations (3.5). All quantities here are attributed to the centroidal co-ordinate axes of corresponding cross-sections of an element. The linear distribution of section parameters in matrix $\overset{\circ}{\mathbf{J}}_i$ and vector $\Delta \overset{\circ}{\mathbf{R}}_i$ over the length of an element is assumed, hence, the integration in (3.11) can be performed analytically. The matrix in quadratic brackets is the element stiffness matrix, the integral in the second term of (3.11) represents a certain fictitious element force vector due to the previous stress action. The analytical expressions for the entries of the element stiffness matrix and the components of fictitious element force vector are presented in the Appendix.

The variable u_3 can be eliminated from the element equations (3.11), using the ordinary variable condensation techniques. Elimination formulas are also presented in the Appendix. The variables u_3 will not appear in global finite element equations.

Location of the incremental centroidal axis $\overset{\circ}{x}$ of the element, that is determined by the centroids of the end sections, does not coincide with the origin of the local element co-ordinate axes, chosen initially.

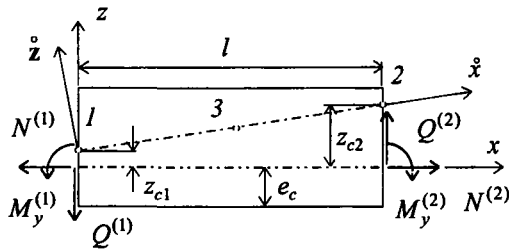


Fig. 3.1. Initial reference axes $x - z$ and incremental shifted reference axes $\overset{\circ}{x} - \overset{\circ}{z}$ of a finite element

This situation is depicted in Fig. 3.1. The stiffness matrix of an element must be computed in regard of the inclined local centroidal axes $\overset{\circ}{x} - \overset{\circ}{z}$, and so the congruent transform of the element stiffness matrix must be performed, to convert it into the initial reference axes $x - z$. This transform consists of the

shift of the nodal points in z direction and the rotation of the initial x -axis to the position $\overset{\circ}{x}$ by the angle β :

$$\tan \beta = \frac{z_{c2} - z_{c1}}{l}. (3.12)$$

On the other hand, the section stress resultants are evaluated in the initial axes, and so the nodal force in the additional node 3 must also be transformed into $\overset{\circ}{x} - \overset{\circ}{z}$, reference axes, as it is stated in the Appendix.

Performing the above-mentioned transforms, one obtains a quasi-elastic stiffness matrix \mathbf{k}_i^e for the e -th finite element at the i -th time step. This matrix is related to the linearized part of strain. To evaluate the contribution of the non-linear large-displacement component of strain, the geometrical stiffness matrix \mathbf{k}_g^e [19] must be added. The incremental linear equations for an individual finite element will read:

$$(\mathbf{k}_i^e + \mathbf{k}_g^e) \Delta \mathbf{z}_i^e = \Delta \mathbf{p}_i^e + \Delta \mathbf{q}_i^e. (3.13)$$

Here $\Delta \mathbf{z}_i^e$ is an incremental displacement vector, $\Delta \mathbf{p}_i^e$ — an incremental vector of externally applied forces; vector $\Delta \mathbf{q}_i^e$ represents the element force increment due to the previous stress action. The global incremental equations for the i -th displacement increment of a whole structure

$$\mathbf{K}_i \Delta \mathbf{z}_i = \Delta \mathbf{P}_i + \Delta \mathbf{Q}_i (3.14)$$

are obtained by means of usual element assemblage formulas

$$\mathbf{K}_i = \sum_e \mathbf{A}_e^t \mathbf{k}_i^e \mathbf{A}_e, (3.15)$$

$$\Delta \mathbf{P}_i = \sum_e \mathbf{A}_e^t \Delta \mathbf{p}_i^e, \quad \Delta \mathbf{Q}_i = \sum_e \mathbf{A}_e^t \Delta \mathbf{q}_i^e, (3.16)$$

$$\Delta \mathbf{z}_i^e = \mathbf{A}_e \Delta \mathbf{z}_i, \quad e = 1, 2, \dots (3.17)$$

Here \mathbf{A}_e is a matrix, relating the e -th individual displacement vector of an element to the global displacement vector of the structure.

4. Non-Linear Solution Program

The set of non-linear structural equations, depending on time, appear for the whole structure. These equations determine the time-varying materially and geometrically non-linear deformation

of a structure. Sophisticated computer program, based on the incremental/iterative Newton-Raphson method has been developed to solve this problem. The load incrementation steps match with the time subdivision points. Each incrementation step consists of two stages: 1) tangent prediction of displacement increments, 2) iterative correction of the obtained tangent solution. At the first stage the tangent solution

$$\Delta \mathbf{z}_i = \mathbf{K}_i^{-1}(\Delta \mathbf{P}_i + \Delta \mathbf{Q}_i) \quad (4.1)$$

is performed at every time/load incrementation step. The global displacement vector $\mathbf{z}_i = \mathbf{z}_{i-1} + \Delta \mathbf{z}_i$, obtained after the current step, generally will not satisfy global non-linear equations. The arising error can be described in a linearized form, and the recurrent matrix equation for the equilibrium corrections may be written:

$$\mathbf{K}_i^{(j)} \Delta \mathbf{z}_i^{(j)} = \mathbf{P}_i - \mathbf{F}(\mathbf{z}_i^{(j-1)}), \quad j = 1, 2, \dots \quad (4.2)$$

The right-hand side of this equation can be considered as certain nodal force unbalance vector. \mathbf{P}_i here is the external force vector at the i -th time step, and $\mathbf{F}(\)$ is the nodal force vector at the same time, corresponding to the nodal displacements $\mathbf{z}_i^{(j-1)}$, that are obtained after $j-1$ equilibrium correction steps. Nodal force vector is determined in the initial co-ordinate axes, and there is no need to transform it, but the third-node axial force component must be represented in $\hat{x}-\hat{z}$, axes, using equations (A.5), (A.6). Vector $\Delta \mathbf{Q}_i$, representing the action of previous stress history, does not appear in this equation. It must be noted that the correction value $\Delta \mathbf{z}_i^{(j)}$ do not correspond to any time interval; it is the j -th addition to the approximate displacement vector value $\mathbf{z}_i^{(j-1)}$ at just the same time moment t_i .

The computer program comprises a number of levels: 1) modelling of individual concrete layers of reinforced concrete cross-sections, 2) evaluating the quasi-elastic incremental stiffness parameters and stress resultants of the cross-sections, 3) computing incremental stiffness matrices and stress resultants of the finite elements, 4) the global analysis of non-linear behaviour of a whole structure.

Numerical procedure for a separate layer or fibre of concrete is described in [14]. The array of stress

history of a fibre $\sigma(t)$ must be supplied for this procedure. The stress values are saved indirectly, as the functions of the strain parameters ε_i^s according to (2.1). The potential advantage of this way of storing is that it utilises the linear distribution of strains over the height of the cross-section, and cross-sectional distribution of stresses may be represented more economically in this way [15]. The procedure computes the quasi-elastic modulus \tilde{E}_i , the strain increment due to previous stress action $\Delta \varepsilon_i'$ for every time step, and updates the stress value $\sigma(t_i)$ by the end of the current time step. This procedure also detects possible unloading/reloading of the concrete fibre. The quasi-elastic modulus is $\tilde{E}_i = E_{sec}$, if the concrete fibre is uncracked, or if unloading takes place. Otherwise the modulus \tilde{E}_i corresponds to a quantity in brackets of (2.5)

$$\frac{1}{\tilde{E}_i} = \frac{1}{E_{tan}} - \frac{1}{E_{sec}} + \frac{1}{E_i'} \quad (4.3)$$

Numerical procedures of the second level compute the integral quantities (3.1) – (3.3) for the reinforced concrete cross-section at the i -th time step. These quantities represent incremental stiffness parameters J_{00}, J_{0y}, J_{yy} , section stress resultants F, M_y , and incremental components $\Delta F', M_y'$ of these resultants due to the previous stress action. This procedure uses the values of \tilde{E}_i , $\Delta \varepsilon_i'$, and $\sigma(t_i)$, computed by the first-level procedure.

The third-level procedures present incremental stiffness matrix \mathbf{k}_i^e and fictitious force increment $\Delta \mathbf{q}_i^e$ for each individual finite element e before the current i -th time step, and the nodal force resultants after the current time step. Geometric stiffness matrix for each finite element is added according to [19].

Incremental/iterative Newton - Raphson procedure is employed in the fourth level. Updated Lagrangian approach was used. External loading is given as a function of time. The global displacement incrementation procedure is performed as follows:

1. Input: time subdivision points t_i , external forces F_i , $i = 0, 1, \dots, N$.
2. Loop over the time increments: $i = 1, \dots, N$.
3. Compute and factorize incremental stiffness matrix of the structure.

4. Compute previous load action parameters (3.3) and add them to the load increment at a current time step.
5. Solve incremental equations for displacement increments.
6. If unloading is detected anywhere, modify the stiffness parameters of the corresponding concrete layer and return to the previous time step $i = i - 1$; go to 3.
7. Equilibrium iteration loop: $j = 1, 2, \dots$
8. Update: configuration, element deformations.
9. Compute and factorize incremental stiffness matrix of the structure.
10. Compute unbalanced nodal forces.
11. If the norm of unbalanced forces does not exceed the tolerance, complete the equilibrium iterations.
12. Solve incremental equations for displacement corrections.
13. End of the equilibrium iteration loop.
14. If the lifespan of the structure is over, complete the incrementation loop.

The program is written in FORTRAN 77, and works on PENTIUM personal computer. The software can be easily modified to adopt any analytical expression for creep law and for cracking relations of reinforced concrete. The further development is also possible, introducing the assessment of quasi-brittle behaviour of concrete in the compression zone.

5. Numerical Results

The non-linear analysis of a frame, presented in the Fig. 5.1, was performed, using the program. The loading of the frame is growing from zero, attains its final level at time moment $t = 316.6$ days, and remains constant until the end of a lifetime of a structure $t_N = 10000$ days. The concrete strength in compression is 30.0 MPa, tensile strength of concrete, computed by the empirical formula [20], is

$$f_t' = 0.324 \sqrt[3]{f_c^2} = 3.128 \text{ MPa}$$

modulus of elasticity of steel reinforcement is $E_s = 200000$ MPa. Detailed description of concrete mix composition used here can be found in the preceding publication [15].

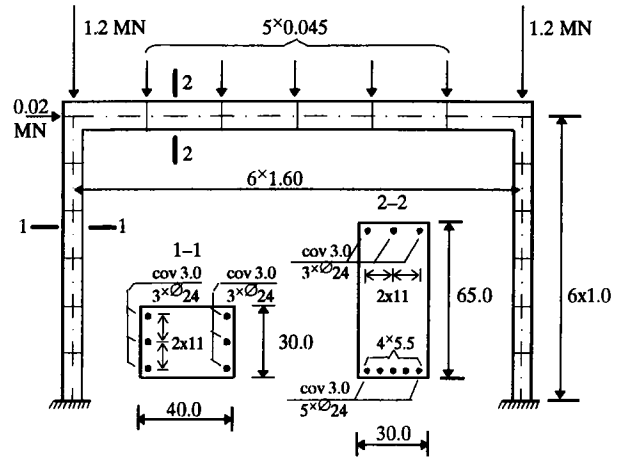


Fig. 5.1. Finite element model of the frame

The creep compliance function $J(t, t')$ for concrete was represented analytically according to [6]. Time-dependent elastic properties of concrete can be described by the conventional short-time elastic modulus corresponding to load duration of about $\Delta t = 0.1$ day

$$E(t) = 1/J(t + \Delta t, t)$$

and by the creep coefficient

$$\phi(t, t') = E(t') J(t, t') - 1.$$

These quantities are plotted on the Fig. 5.2.

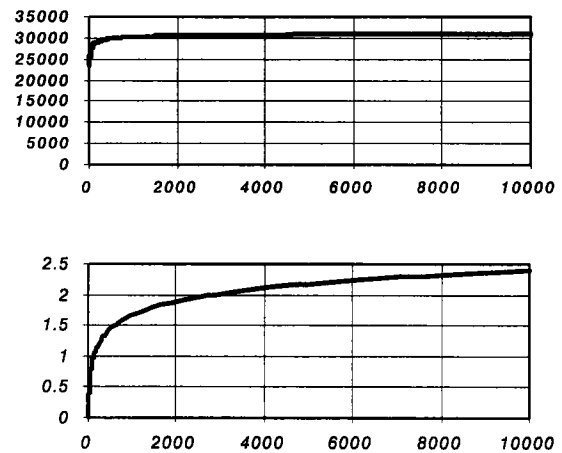


Fig. 5.2. Short-time elastic modulus (upper graph) and creep coefficient $\phi(t, t')$, corresponding to the time of loading $t = 10.0$ days (lower graph).

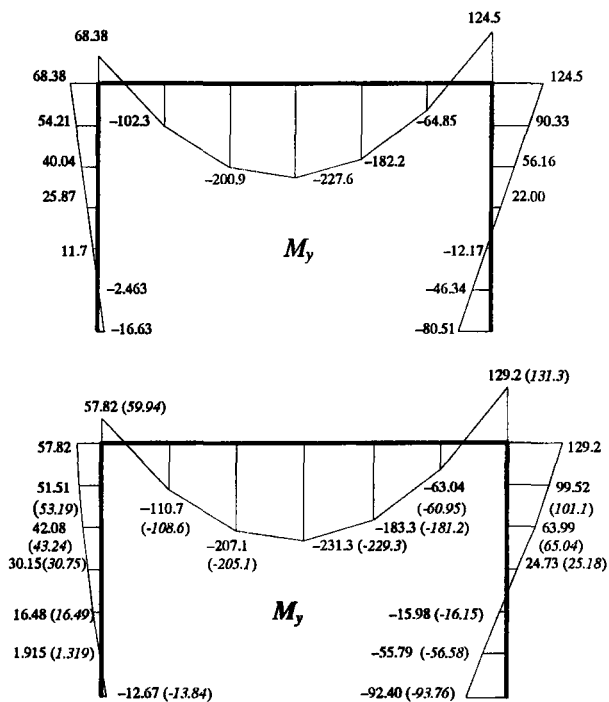


Fig. 5.3. Redistribution of bending moments at time $t=10000$ days. Bending moments: when geometrical non-linearity is neglected (upper graph); in lower graph geometrical non-linear solution is shown. In brackets are written bending moments with the account of the reloading effect

In Fig. 5.3 there are plotted the final values of bending moments. The influence of slenderness and unloading effects is clearly seen in this figure.

Fig. 5.4 shows the stresses (on the left) and strains (on the right) of the middle cross-section of the frame, for time $t=20.0$ days, when the loading attains its full magnitude, and for the final time moment $t=10000.0$ days. The fine line represents stresses and strains that are obtained, neglecting the unloading effect, and the bold line shows the strict solution.

The difference of the stress history of concrete for the separate layer of the middle section is seen on the Fig. 5.5. Bold lower line shows the true stress history, including reloading effects, the upper line is obtained neglecting the reloading effects.

7. Summary and conclusions

The consistent geometrically and materially non-linear finite element algorithm is presented, and appropriate computer code, applicable to creep and large displacement analysis of plane reinforced concrete frame structures, has been written and tested.

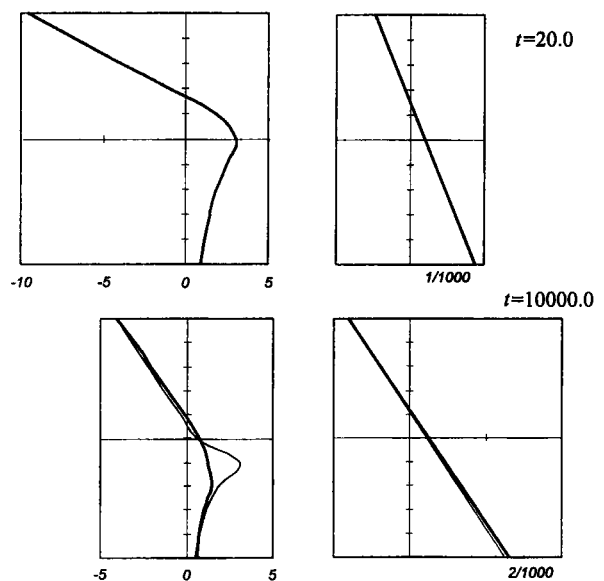


Fig. 5.4. Stresses and strains of the middle cross-section

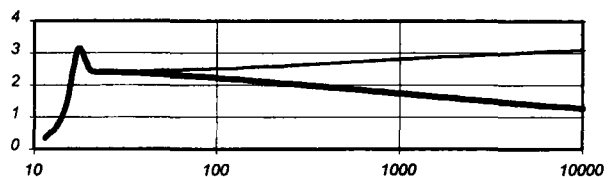


Fig. 5.5. Stress history for the layer $y = -0.0325$ m of the middle cross-section of the frame

Memory model of concrete creep has been successfully introduced into the algorithm. Possible cracking of the tension zone and reloading effects are taken into account. The layer representation of a cross-section is used. The method is free of simplifying assumptions regarding the creep theory and non-linear material behaviour. The algorithm used can be developed further, it allows to account for non-linear quasi-brittle behaviour and non-linear creep effects in the compression zone and the plasticity of steel reinforcement, as well. The numerical algorithm showed its stability in case of unloading of certain concrete layers. Sufficient accuracy can be achieved subdividing the section into 20 to 50 layers and introducing about 50 time intervals over the lifespan of a structure.

References

1. Bažant Z. P. Prediction of Concrete Creep Effects Using Age-Adjusted Effective Modulus Method // ACI Journal, Vol. 69, No. 4, Apr. 1972, p. 212-217.
2. R. Gaiotti, B. S. Smith. P-Delta Analysis of Building Structures // Journal of Structural Engineering, Vol. 112, No. 10, Oct. 1989, p. 755-770.

3. B. Massicotte, A. E. Elwi, J.G. MacGregor. Tension Stiffening Model for Planar Reinforced Concrete Members // *Journal of Structural Engineering*, ASCE, Vol. 116, No. 8, Nov. 1990, p. 3039–3058.
4. ACI Committee 209. Prediction of creep, shrinkage and temperature effects in concrete structures // *ACI manual of concrete practice*. Part I. American Concrete Institute (ACI), Detroit, Mich., 1990.
5. British Standards Institution. Eurocode 2: Design of Concrete Structures — Part 1. General Rules and Rules for Buildings. BSI, London, 1992, DD ENV 1992–1–1: 1992.
6. Z.P. Bažant, J.-K. Kim. Improved Prediction Model for Time-Dependent Deformations of Concrete // *Materials and Structures*. Part 1 — Shrinkage, Vol. 24, 1991, p. 327–345, Part 2 — Basic Creep, Vol. 24, 1991, p. 409–421, Part 3 — Creep at Drying, Vol. 25, 1992, p. 21–28, Part 4 — Temperature Effects, Vol. 25, 1992, p. 84–94, Part 5 — Cyclic Load and Cyclic Humidity, Vol. 25, 1992, p. 163–169, Z. P. Bažant, L. Panula, J.-K. Kim, Y. Xi. Part 6 — Simplified Code-Type Formulation, Vol. 25, 1992, p. 219–223.
7. A. Kawano, R.F. Warner. Model Formulation for Numerical Creep Calculations for Concrete // *Journal of Structural Engineering*, Vol. 122, No. 3, Mar. 1996, p. 284–290.
8. L. Dezi, G. Leoni, A.M. Tarantino. Algebraic Methods for Creep Analysis of Continuous Composite Beams // *Journal of Structural Engineering*, Vol. 122, No. 4, Apr. 1996, p. 423–430.
9. Рекомендации по учету ползучести и усадки бетона при расчете бетонных и железобетонных конструкций. НИИЖБ Госстроя СССР. Москва: Стройиздат, 1988. 120 с.
10. Z.P. Bažant, S. Prasannan. Solidification Theory for Concrete Creep. I: Formulation. II: Verification and Application // *Journal of Engineering Mechanics*, ASCE, Vol. 115, No. 8, Aug. 1989, p. 1691–1725.
11. M.A. Bradford, R. I. Gilbert. Non-Linear Time-Dependent Behaviour of Slender Concrete-Filled Rectangular Steel Columns // *Proceedings of the Institution of Civil Engineers. Structures & Buildings*, Vol. 94, May 1992, p. 179–186.
12. S.E. Gutiérrez, R. O. Cudmani, R. F. Danesi. Time-Dependent Analysis of Reinforced and Prestressed Concrete Members // *ACI Structural Journal*, Vol. 93, No. 4, July–Aug. 1996, p. 420–427.
13. Z. P. Bažant, B. H. Oh. Deformation of Progressively Cracking Reinforced Concrete Beams // *ACI Journal*, Vol. 81, No. 3, May–June 1984, p. 268–278.
14. I. Cypinas. Numerical Modelling of Reinforced Concrete Creep in the Tension Zone // *Building Construction*. 1996, No. 2(6), p. 6–12.
15. I. Cypinas. Numerical Modelling of Reinforced Concrete Members in Flexure // *Building Construction*. 1996, No. 3(7).
16. G. K. V. Prakhya, C. T. Morley. Tension Stiffening and Moment-Curvature Relations for Reinforced Concrete Elements // *ACI Structural Journal*, Vol. 87, No. 5, Sep.-Oct. 1990, p. 597–605.
17. R. De Borst. Smeared Cracking, Plasticity, Creep, and Thermal Loading — a Unified Approach // *Computer Methods in Applied Mechanics and Engineering*, Vol. 62, No. 1, 1987, p. 89–110.
18. S. Cognini, L. Dezi, G. Mendito, E. Speranzini. Viscoelastic Moment-Curvature Diagrams // *ACI Materials Journal*, Vol. 84, No. 6, Nov.-Dec. 1987, p. 519–524.
19. J.H. Argyris, O. Hilpert, G.A. Malejannakis, D.W. Scharpf. On the Geometrical Stiffness of a Beam in Space — a Consistent V. W. Approach // *Computer Methods in Applied Mechanics and Engineering*, Vol. 20, 1979, p. 105–132.
20. M. Raphael. Tensile Strength of Concrete // *ACI Journal*, Vol. 81, No. 2, Mar.-Apr. 1984, p. 158–165.

Appendix

The elements of the incremental element stiffness matrix k^u , related to the longitudinal displacements in regard of the centroidal axis:

$$\begin{aligned}
 k_{11}^u &= \frac{1}{3L}(7J_{00} + 1.5\Delta J_{00}), & k_{12}^u &= \frac{1}{3L}(J_{00} + 0.5\Delta J_{00}), \\
 k_{13}^u &= -\frac{1}{3L}(8J_{00} + 2\Delta J_{00}), \\
 k_{22}^u &= \frac{1}{3L}(7J_{00} + 5.5\Delta J_{00}), & k_{23}^u &= -\frac{1}{3L}(8J_{00} + 6\Delta J_{00}), \\
 k_{33}^u &= \frac{1}{3L}(16J_{00} + 8\Delta J_{00}). & & (A.1)
 \end{aligned}$$

Here $J_{00} = J_{00}^{(1)}$, $\Delta J_{00} = J_{00}^{(2)} - J_{00}^{(1)}$, where $J_{00}^{(1)}$ and $J_{00}^{(2)}$ are the values, computed at the nodes 1 and 2 respectively. These quantities are referred to the plane, perpendicular to the inclined centroidal \hat{x} -axis, L the length of the element in \hat{x} direction.

After the elimination of the displacement u_3 the condensed matrix \hat{k}^u consists of the elements

$$\begin{aligned}
 \hat{k}_{11}^u &= k_{11}^u - k_{13}^u k_{31}^u / k_{33}^u, & \hat{k}_{12}^u &= k_{12}^u - k_{13}^u k_{23}^u / k_{33}^u, \\
 \hat{k}_{22}^u &= k_{22}^u - k_{23}^u k_{32}^u / k_{33}^u. & & (A.2)
 \end{aligned}$$

The elements of the bending part of the matrix, related to the nodal displacements w_1, χ_1, w_2, χ_2 , are

$$\begin{aligned}
 k_{11}^b &= \frac{12}{L^3} \left(J_{yy} + \frac{1}{2} \Delta J_{yy} \right), & k_{12}^b &= -\frac{6}{L^2} \left(J_{yy} + \frac{1}{3} \Delta J_{yy} \right), \\
 k_{13}^b &= -k_{11}^b, & k_{14}^b &= -\frac{6}{L^2} \left(J_{yy} + \frac{2}{3} \Delta J_{yy} \right), \\
 k_{22}^b &= \frac{4}{L} \left(J_{yy} + \frac{1}{4} \Delta J_{yy} \right), & k_{23}^b &= -k_{12}^b, \\
 k_{24}^b &= \frac{2}{L} \left(J_{yy} + \frac{1}{2} \Delta J_{yy} \right),
 \end{aligned}$$

$$k_{33}^b, k_{34}^b = -k_{14}^b, \quad k_{44}^b = \frac{4}{L} \left(J_{yy} + \frac{3}{4} \Delta J_{yy} \right). \quad (\text{A.3})$$

Here J_{yy} and ΔJ_{yy} are defined analogically, as J_{00} and ΔJ_{yy} , and matrix is defined in the $\hat{x} - \hat{z}$ axes.

The upper symmetric triangle of the whole matrix is

$$\mathbf{k}^e = \begin{bmatrix} \hat{k}_{11}^u & 0 & 0 & \hat{k}_{12}^u & 0 & 0 \\ & k_{11}^b & k_{12}^b & 0 & k_{13}^b & k_{14}^b \\ & & k_{22}^b & 0 & k_{23}^b & k_{24}^b \\ & & & \hat{k}_{22}^u & 0 & 0 \\ & & & & k_{33}^b & k_{34}^b \\ & & & & & k_{44}^b \end{bmatrix} \quad (\text{A.4})$$

The components of section force resultant vector, Fig. 3.1, are obtained in initial reference axes, and they must be recalculated to the $\hat{x} - \hat{z}$ reference axes:

$$\left. \begin{aligned} \dot{N} &= N \cos \beta + Q \sin \beta, \\ \dot{Q} &= -N \sin \beta + Q \cos \beta. \end{aligned} \right\} \quad (\text{A.5})$$

The nodal forces, related to the degrees of freedom u_1, u_2, u_3 , are found by the formulas that are derived from the equation (3.8), using the principle of virtual displacements:

$$\begin{aligned} \dot{F}'_1 &= -\frac{5}{6} \dot{N}^{(1)} - \frac{1}{6} \dot{N}^{(2)}, & \dot{F}'_2 &= \frac{1}{6} \dot{N}^{(2)} + \frac{5}{6} \dot{N}^{(1)}, \\ \dot{F}'_3 &= \frac{2}{3} (\dot{N}^{(1)} - \dot{N}^{(2)}). \end{aligned} \quad (\text{A.6})$$

Here $\dot{N}^{(1)}$ and $\dot{N}^{(2)}$ are stress resultants according to (A.5), computed at the corresponding end nodes of an element. The eliminated displacement u_3 is determined by the formula

$$u_3 = (F'_3 - k_{31}^u u_1 - k_{32}^u u_2) / k_{33}^u \quad (\text{A.7})$$

that follows directly from the element force equations. This quantity is used to compute the strains in element nodes according to (3.8).

Įteikta 1996 10 20

GEOMETRIŠKAI NETIESINIS GELŽBETONINIŲ RĖMŲ SKAIČIAVIMAS, ATSIŽVELGIANT Į VALKŠNUMĄ IR PLYŠIUS TEMPIAMOJOJE ZONOJE

I. Cypinas

Santrauka

Sukurtas netiesinis skaičiavimo metodas ir sudaryta kompiuterio programa, kuri įgalina atlikti realių statybinių konstrukcijų valkšnumo skaičiavimą, veikiant ilgalaikėms apkrovoms ir esant plyšiams tempiamoje betono zonoje. Programa sprendžia netiesinę rėmo deformacijos lygčių sistemą Niutono-Rafsono metodu. Naudojamas geometriškai ir fiziškai netiesinis baigtinių elementų metodo algoritmas. Betonui priimamas integralinis valkšnumo dėsnis, gniuždymo zonai apsiribojama tiesiniu valkšnumu, tempiamam betonui taikomas analitinis modelis, kurį sudaro pleišėjantis betono elementas su krentančia įtempimų-deformacijų kreivės šaka, nuosekliai sujungtas su tiesiškai deformuojamu valkšniu nesupleišėjusio betono elementu. Sluoksninis skerspjūvio modelis įgalina taip pat ir gniuždymo zonai pritaikyti netiesinį deformavimo dėsnį. Uždavinys yra sprendžiamas skaičiuojant deformacijų ir poslinkių prieaugius mažais laiko žingsniais.

Igoris CYPINAS. Doctor, Associate Professor. Kaunas University of Technology. Department of Structural Engineering. 48 Studentų St, 3031 Kaunas.

In 1957 he completed road engineering studies at Kaunas University of Technology (the former Kaunas Polytechnical Institute). Doctor's degree in structural mechanics at the same University in 1966. Since 1963 with small interruptions he works at Kaunas University of Technology. Research interests: non-linear and time-dependent structural analysis, finite element programming, structural stability and optimisation.